# Raman Performance Characteristics of Teflon®-AF 2400 Liquid-Core Optical-Fiber Sample Cells

**ROBERT ALTKORN,* ILIA KOEV,* and MICHAEL J. PELLETIER***

*Department of Physics and Astronomy, Northwestern University, 1801 Maple Ave., Evanston Illinois 60201 (R.A.); Biogeneral Inc., 9925 Mesa Rim Road, San Diego, California 92121 (I.K.); and Kaiser Optical Systems Inc., 371 Parkland Plaza, Ann Arbor, Michigan 48103 (M.J.P.)*

**Several properties of Teflon®-AF liquid-core optical-fiber (LCOF) sample cells relevant to their utility in analytical Raman spectroscopy have been investigated. These include the nature and extent of cladding-related background and its effect on signal-to-noise ratio, and the dependence of intensity enhancement on LCOF length, core diameter, excitation wavelength, and scattering wavelength. Significant improvements in signal-to-noise ratio relative to conventional sampling techniques were demonstrated in LCOFs filled with dilute ($6 \times 10^{-2}$ M and $6 \times 10^{-4}$ M) aqueous solutions of phenylalanine. A maximum intensity enhancement factor of approximately 120 was measured by using 50 μm i.d. LCOFs filled with methanol and 532 nm excitation. Enhancement in 785 nm-excited spectra was found to vary with Raman shift in a manner consistent with self-absorption by high-overtone vibrational bands in the core liquid.**

Index Headings: **Raman spectroscopy; Teflon®-AF; Liquid-core optical fiber; Waveguide capillary cell; Liquid-core waveguide.**

## INTRODUCTION

The ability of liquid-core optical-fiber (LCOF) sample cells to significantly enhance both the intensity and signal-to-noise ratio of spontaneous Raman spectra was first demonstrated by Walrafen and Stone in the early 1970s.[1] Using 75 μm i.d. fused-quartz capillaries up to 25 meters in length filled with benzene and tetrachloroethylene, they reported intensity enhancements of as much as 3000 relative to conventional sampling arrangements and the detection of a number of previously unseen bands. Subsequently, Walrafen[2-4] and other workers[5-13] used glass- and fused-silica-clad LCOFs to acquire Raman spectra of a variety of high-refractive-index liquids. However, in spite of demonstrated optical advantages, LCOF sampling has yet to achieve widespread popularity in Raman spectroscopy. This circumstance is due in large part to the fact that the high refractive index of silica ($n = 1.46$), coupled with the requirement for total internal reflection that the refractive index of the core exceed that of the cladding, severely limits the choice of core liquids. Most liquids of analytical interest, including the vast majority of aqueous solutions, have refractive indices well below that of silica.

Walrafen and Stone recognized the limitations imposed by silica-based glasses and recommended the use of low-refractive-index materials, such as Teflon®,[1] to extend LCOF sampling to a wider range of liquids. However, at the time of their work Teflon® capillaries of suitable optical quality were unavailable.[2] Within the last six years, a number of LCOFs capable of guiding light through water ($n = 1.33$) have been fabricated from the clear, amorphous, low-refractive-index ($n = 1.29$–$1.31$[14]) copolymers of 2,2-bistrifluoromethyl-4,5-difluoro-1,3-dioxole and tetrafluoroethylene sold by DuPont under the trade name Teflon®-AF. LCOFs based on plastic and glass capillaries coated internally with Teflon®-AF,[15-19] glass capillaries coated externally with Teflon®-AF,[20,21] and capillaries made entirely of Teflon®-AF[22-26] have been reported. Quite recently, the ability of Teflon®-AF-based LCOFs to enhance the intensity of spontaneous Raman spectra of low-refractive-index liquids has been demonstrated.[22,25] In the present paper we address several issues relevant to the practical application of liquid-core Teflon®-AF fibers in Raman spectroscopy. In particular, we consider the dependence of intensity enhancement on LCOF length and diameter, the extent of fluorescent and Raman background generated in the LCOF wall and their effect on signal-to-noise ratio, and the dependence of both intensity and signal-to-noise enhancement on excitation wavelength.

## EXPERIMENTAL

**LCOF Fabrication.** The Teflon®-AF 2400 capillary tubing used in this work was manufactured by a technique described previously.[22] The tubing was water-clear and highly flexible. Loss measurements were performed on several samples of tubing ranging in inside diameter from 50 to 355 μm. Raman experiments were conducted with 50 μm i.d. × 200 μm o.d. and 150 μm i.d. × 400 μm o.d. tubing.

LCOFs were formed by mounting the Teflon®-AF tubing in end cells similar to those described previously.[20] The end cells are based on standard 1/16 in HPLC tees fitted with small adapters having interior diameters slightly larger than the outer diameter of the tubing and terminating in 150 μm thick fused-silica windows. The adapters used in this work were somewhat larger than the SMA-connector-based devices described previously and use O-ring seals rather than epoxy, thereby allowing the windows to be removed for cleaning. Light was launched into the proximal end of the LCOF simply by focusing through the window. Liquid was introduced into the LCOF with the use of a peristaltic pump fitted with silicone rubber tubing. In most cases only a single end cell was used; the distal end of the LCOF was placed in a waste receptacle, or, in the case of loss measurements, in a small windowed receptacle attached to a power meter.

**Loss Measurements.** The loss characteristics of LCOFs ranging in inside diameter from 50 to 355 μm were measured at 532 nm with a low-power frequency-

Received 11 February 1999; accepted 6 May 1999.
* Authors to whom correspondence should be sent.


0003-7028/99/5310-1169$2.00/0

doubled diode-pumped YAG laser (MeshTel-Intelite Mesh 101-GM32) and a power meter (Newport Model 815). In all cases, the LCOFs were filled with methanol (Fisher Optima), which was pumped continuously throughout the measurement process by using a peristaltic pump fitted with silicone rubber tubing. The methanol was used as received, without further purification of filtering. Light was launched into the LCOFs with the use of a 10×, 0.25 NA (numerical aperture) microscope objective. The measured full angle of divergence of the laser light was approximately 6°. The relative positions of the laser and objective were kept the same between measurements to ensure that the same launch numerical aperture was used with each LCOF. Unlike previous work in which loss was measured by adjusting the position of a solid silica optical fiber inside the liquid-core fiber,[20,22] all measurements reported here were performed by using a cutback method[27] in which the length of the LCOF was successively reduced through a series of cuts. Although it is destructive, the cutback method was adopted because of the difficulty of finding and working with silica fibers small enough to fit inside 50 μm i.d. LCOFs and to ensure uniformity between measurements. The loss measurements were performed on LCOFs ranging in length from approximately 55 to 95 cm, which were subsequently cut in 5 to 10 cm increments with a scalpel. The position of the proximal end of the LCOF was adjusted prior to the start of each measurement sequence to maximize transmitted laser intensity. Measurements of emitted power were made prior to cutting the full-length LCOF and subsequent to each cut. Attenuation (dB) was calculated on the basis of the ratios of the power emitted from the LCOF after each successive cut to the power emitted after the final cut. Loss (dB/m) and standard deviation were determined by linear least-squares fit to the attenuation vs. length data.

**Raman Measurements.** Raman spectra were measured with two Kaiser Optical Systems HoloLab 5000 Raman microscopes. One Raman microscope was optimized for 532 nm excitation and the other for 785 nm excitation. The HoloLab 5000 Raman microscope consisted of an integrated Raman spectrometer system interfaced to an Olympus BX-60 microscope using a fiber-optic probehead. The integrated Raman spectrometer system,[28] the fiber-optic probehead,[28,29] and the microscope interface[30] have been described previously. Briefly, laser light from the integrated Raman spectrometer system was delivered to the fiber-optic probehead through a 50 μm core diameter graded index (GI) optical fiber. The probehead spectrally filtered the laser light to remove Raman light and luminescence generated in the optical fiber. The filtered laser light was collimated and delivered to the microscope interface. The microscope interface delivered the collimated laser light through the infinity-corrected objective lens of the microscope and into the LCOF. The interface also included a video camera that provided a real-time image of the face of the LCOF and the focused laser spot on the LCOF entrance window.

Light scattered from the LCOF followed the laser light path back into the probehead where the Raman scattered light was separated from the laser light and injected into a single 1.9 m long, 0.27 NA 100 μm core diameter GI optical fiber with the use of a 10×, 16 mm effective focal length (EFL) microscope objective. This optical fiber delivered the Raman scattered light to an axial transmissive spectrograph[31] inside the integrated Raman spectrometer. The spectrograph used a 50 μm entrance slit, a holoplex transmission grating,[32] and an 85 mm focal length lens to focus the Raman spectrum onto a charge-coupled device (CCD) detector. The linear dispersion was 2.5 $cm^{-1}$ per detector pixel for the 532 nm system and 2.0 $cm^{-1}$ per detector pixel for the 785 nm system. The holoplex transmission grating split the Raman spectrum in half and stacked the halves on top of each other at the CCD detector, allowing simultaneous acquisition of the entire Raman spectrum (spectral coverage 100 to 4400 $cm^{-1}$ for 532 nm excitation and 100 to 3500 $cm^{-1}$ for 785 nm excitation).

Each Raman microscope was calibrated in wavelength to sub-pixel accuracy by fitting a neon emission spectrum from a Kaiser Optical Systems external calibration accessory to a third-order polynomial[33] using HoloGrams software. The exact laser wavelength was then determined from a cyclohexane spectrum with the use of the band position values published by Fountain et al.[34] The intensity axis of the 532 nm Raman microscope was corrected with the use of the NIST-traceable incandescent source in a Kaiser Optical Systems external calibration accessory. The incandescence spectrum was blackbody-corrected in photons per wavenumber. Intensity axis correction for the 785 nm microscope was not available.

All Raman experiments were performed in the backscattering geometry described above. Methanol (Burdick and Jackson high-purity solvent, GC-HPLC grade, $n$ = 1.33) was chosen for the measurements of intensity enhancement because its band system is well suited to analyzing enhancement as a function of Raman shift. It was used as received, without further purification or filtration. Dilute ($6 \times 10^{-2}$ M and $6 \times 10^{-4}$ M) solutions of phenylalanine (Aldrich, 99%) in deionized water (17.3 MΩ cm) were used to study signal-to-noise enhancement. The phenylalanine was used as received. The solutions were passed through a 0.45 μm filter (Gelman PTFE acrodisc) immediately prior to use. The numerical aperture of the LCOFs (approximately 0.3 for both methanol and dilute aqueous solutions) was well matched to the input optic of the 532 nm system (a 10×, 16 mm EFL, 0.3 NA microscope objective), but larger than that of the 785 nm system (a 10×, 16 mm EFL, 0.25 NA objective).

## RESULTS AND DISCUSSION

**Fluorescence/Raman Background.** Spectra of empty Teflon®-AF capillary tubing acquired at 785 nm showed no indication of fluorescence. However, Fig. 1 shows that spectra of the same tubing acquired at 532 nm are dominated by a broad fluorescence peak centered near 1500 $cm^{-1}$. The intensity of this feature was observed to decay significantly on the time scale of minutes under 532 nm irradiation. At this time we are unable to identify the source of fluorescence; however, the presence of similar features in the spectra of raw Teflon®-AF 2400 pellets indicates that it is not created by degradation of the Teflon®-AF during the capillary manufacturing process. The existence of this strong fluorescence peak raises concern about the level of signal-to-noise ratio improvement that

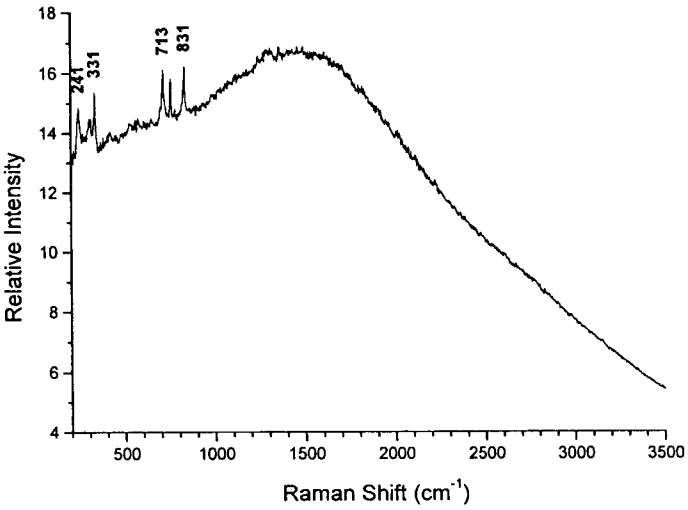


FIG. 1. Spectrum of wall of empty 50 μm i.d., 200 μm o.d. Teflon®-AF 2400 LCOF acquired with 532 nm excitation.

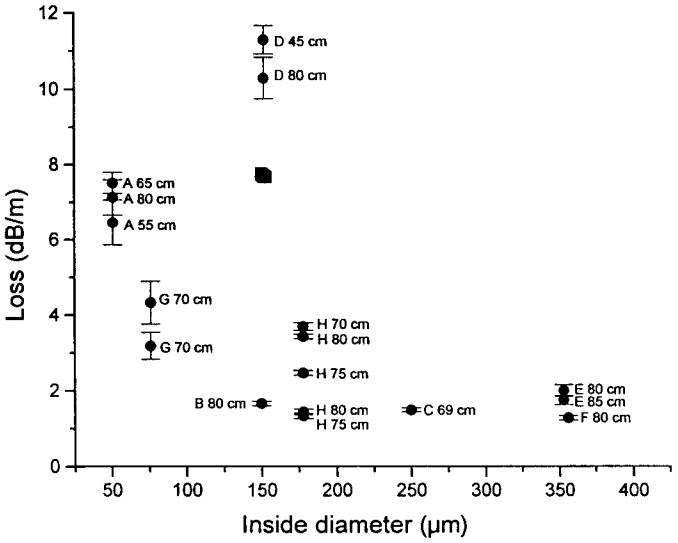


FIG. 2. Loss vs. diameter for methanol-filled LCOFs. The total length of LCOF cut in each measurement is shown in the figure. LCOF wall thicknesses are as follows: (*A*) 75 μm; (*B*) 125 μm; (*C*) 138 μm; (*D*) 280 μm; (*E*) 81 μm; (*F*) 140 μm; (*G*) 64 μm; (*H*) 230 μm.

might be achieved by using Teflon®-AF-based LCOFs. However, as discussed below, the LCOFs were found to provide significant signal-to-noise ratio enhancement despite the presence of this feature. We therefore made no attempt to temporarily or permanently bleach the capillary tubing.

**LCOF Loss.** The loss characteristics of LCOFs of various diameter are shown in Fig. 2. These are, to our knowledge, the only data ever acquired on the variation in loss with diameter for low-refractive-index-core LCOFs. Data points labeled with the same letter correspond to LCOFs fabricated from capillary tubing cut from the same spool. The error bars represent the standard deviation calculated for the individual LCOF on which the loss measurement was performed. Although ray models predict loss that varies inversely with core diameter in cases where reflection loss is the primary source of attenuation[35] (as would be expected here), it is clear from Fig. 2 that factors other than inside diameter can be important in determining loss. Beyond this consideration, the data in Fig. 2 seem to suggest that loss may increase significantly at very small diameters. However, we are hesitant to draw this conclusion without data on LCOFs of similar size made of tubing fabricated in different manufacturing runs and are in the process of preparing more extensive tests. Given that the loss characteristics of LCOFs directly affect Raman signal intensity, we believe that it is worthwhile to (nondestructively) measure loss prior to selecting capillary tubing for use in LCOFs. This approach may be particularly important in quantitative analysis, where the relative contributions of LCOF loss and analyte concentration to observed intensity must be understood.

**Intensity vs. LCOF Length.** The intensity of Raman radiation produced by LCOFs in backscattering geometry has been predicted to vary with LCOF length according to the equation[2]

$$P_R = \frac{P_L K}{2\alpha}(1 - e^{-2\alpha x}) \qquad (1)$$

where $P_R$ is the Raman power, $P_L$ is the laser power, α is the (base-*e*) LCOF loss coefficient, $x$ is the LCOF length, and $K$ is a constant related to the scattering cross section of the core liquid and collection angle inside the LCOF. Equation 1 is based on the assumptions that LCOF loss is characterized by a single exponential and that the loss coefficient is the same for both the laser and Raman scattered radiation. To test the validity of this equation for the Teflon®-AF LCOFs used in this work, we simultaneously measured Raman intensity and transmitted laser intensity as functions of LCOF length for a 150 μm i.d. LCOF using the cutback method. The section of capillary used here was different from that used to obtain the loss data shown in Fig. 2. We used 532 nm rather than 785 nm excitation to avoid high vibrational overtone absorption bands that significantly increase the loss of methanol-filled LCOFs in the near-infrared.[36] The results of this measurement are plotted in Fig. 3, which shows Raman intensity of the 2834 and 2943 cm$^{-1}$ C–H stretching bands in methanol and laser beam attenuation as functions of LCOF length. The solid lines in Fig. 3 rep-

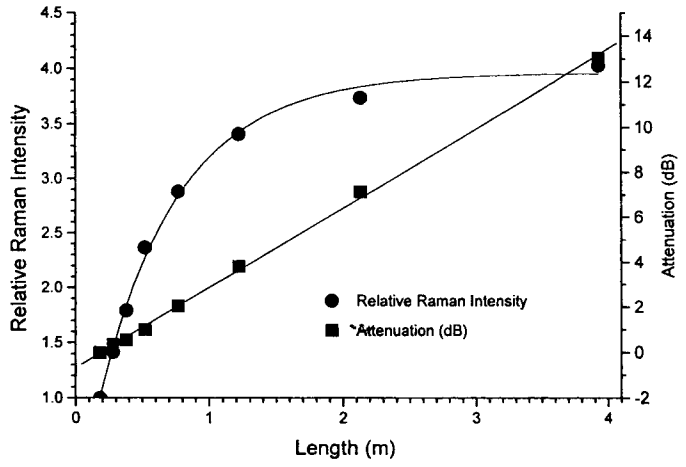


FIG. 3. Raman intensity and 532 nm laser attenuation as functions of LCOF length in 150 μm i.d., 400 μm o.d. Teflon®-AF 2400 LCOF filled with methanol.

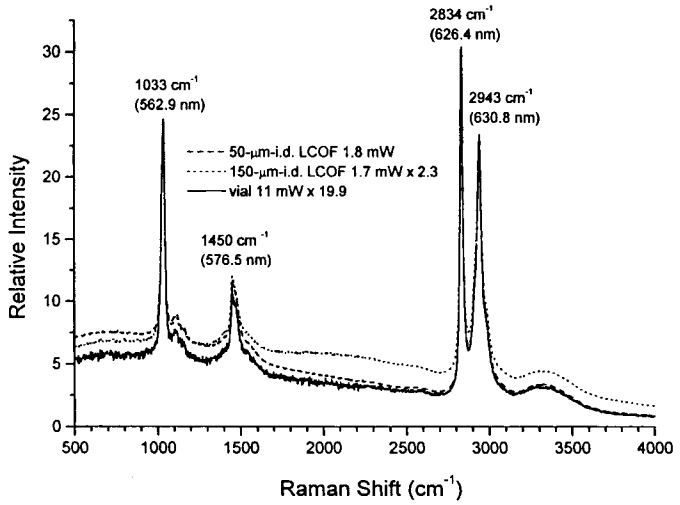


FIG. 4. Spectra of methanol in 98 cm long, 50 μm i.d. LCOF, 393 cm long, 150 μm i.d. LCOF, and vial acquired with 532 nm excitation in single 0.5 second acquisitions. Absolute peak positions are shown in parentheses.

resent linear least-squares fits to the anticipated functional forms of the data (Eq. 1 in the case of Raman intensity and linear increase in the case of laser attenuation). It is seen that both the measured Raman intensity and transmitted laser power conform well to the anticipated functional forms. Further, the loss coefficients calculated from the Raman intensities ($\alpha$ = 0.83 $m^{-1}$ or 3.6 dB/m) and laser transmission measurements ($\alpha$ = 0.81 $m^{-1}$ or 3.5 dB/m) are in good agreement and indicate that this section of capillary has higher loss than that used to obtain the data in Fig. 2.

It is easily seen from Eq. 1 that the Raman intensity produced by an LCOF in backscattering geometry reaches a maximum value of

$$P_{R,Max} = \frac{P_L K}{2\alpha} \tag{2}$$

when the physical LCOF length is much greater than its attenuation length, $x_a$ (distance along the fiber at which the laser intensity falls to $1/e$ of its original value), where

$$x_a = \frac{1}{\alpha}. \tag{3}$$

In order to obtain the maximum possible Raman intensity and avoid intensity variations related to LCOF length, LCOFs at least several times longer than the attenuation length were used in all experiments described below.

**Enhancement vs. LCOF Diameter.** Figure 4 shows spectra of methanol acquired by using 532 nm excitation in (1) a 98 cm long, 50 μm i.d. LCOF, (2) the same 393 cm long 150 μm i.d. LCOF used for the Raman intensity vs. length measurements, and (3) a 3.8 cm deep vial that provided no enhancement through waveguiding. The spectra were obtained with laser power levels of 1.8, 1.7, and 11 mW, respectively, and were scaled by factors of 1, 2.3, and 19.9 respectively, to make the absolute heights of the 2834 $cm^{-1}$ C–H symmetric stretching peaks the same in each spectrum. In all cases the spectra were acquired in a single 0.5-second accumulation. Therefore the approximate intensity enhancement factors relative to the vial are 122 for the 50 μm i.d. LCOF and 56 for the 150 μm i.d. LCOF. (Enhancement factors based on peak heights relative to the spectral baseline are approximately 1% lower in the case of the 50 μm i.d. LCOF and 7% lower for the 150 μm i.d. LCOF.) The power emitted from the distal end of the waveguide was 0.17 mW in the case of the 50 μm i.d. LCOF and 0.05 mW in the case of the 150 μm i.d. LCOF. Loss values calculated from input and output laser power (10.5 dB/m for the 50 μm i.d. LCOF and 3.85 dB/m for the 150 μm i.d. LCOF) are artificially high because they do not account for coupling loss. Nevertheless, they indicate that the loss of the 50 μm i.d. LCOF is greater than that of the 150 μm i.d. LCOF. They also show that both devices were long compared to their respective attenuation lengths.

Three features of Fig. 4 are notable. First, the enhancement factor appears to be wavelength independent in both LCOFs. While this observation is not surprising, it is in distinct contrast to the results that were obtained when 785 nm excitation was used. Second, the baselines of the spectra acquired in the LCOFs appear to be shifted relative to that of the spectrum in the vial. At present we lack a quantitative explanation for this shift. While the spectrum acquired in the 50 μm i.d. LCOF suggests that the baseline might include a component of Teflon®-AF fluorescence, the offset in the spectrum acquired in the 150 μm i.d. LCOF does not appear to follow the profile expected from the fluorescence spectrum in Fig. 1. Finally, it is clear from Fig. 4 that 50 μm i.d. LCOF provided greater intensity enhancement than the 150 μm i.d. LCOF. The fact that the smaller-diameter, higher-loss LCOF provides greater enhancement than the larger LCOF is particularly striking and might seem counterintuitive. We believe that it is due in large part to differences in the efficiencies of coupling light from the LCOFs into the graded-index fiber used to return light to the spectrograph. Unfortunately, several factors complicate quantitative determination of the coupling efficiencies. These include the virtually complete lack of experimental data on the spatial and/or angular dependence of Raman light emitted from any type of LCOF and concomitant difficulty of modeling the coupling process,[37] and the experimental difficulty of measuring the propagation of Raman light through the HoloLab 5000 microscopes. However for a more qualitative estimate of relative coupling efficiencies we can make the following assumptions: (1) The 100 μm core GI fiber that conveys light from the Raman probehead to the spectrograph is the only relevant light-limiting element in the system—that is, light is randomized in this fiber and emerges with the same spatial and angular properties regardless of the source (LCOF) diameter. (2) The microscope images the face of the LCOF onto the face of the GI fiber. (3) The LCOFs are perfectly round, and the Raman output of each LCOF is Lambertian within the solid angle of acceptance of the microscope. And (4) the local NA of the GI fiber is that of a standard parabolic index fiber in which cladding and leaky skew rays can be neglected. Under these assumptions, it can be shown that the ratio of the coupling efficiencies of the two LCOFs to the Raman spectrograph is given by[38]

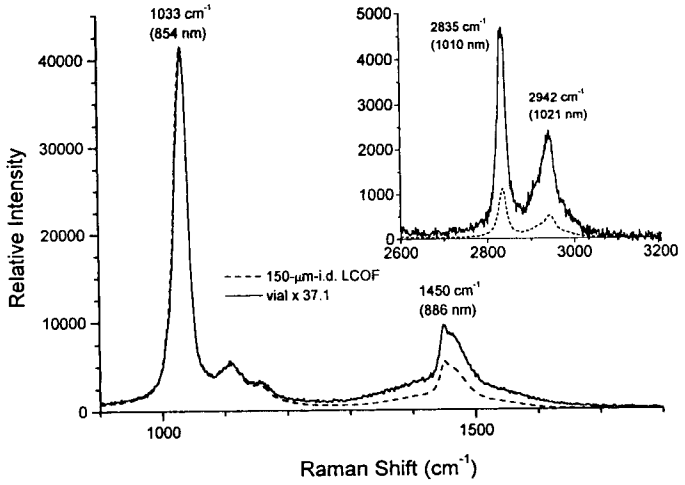


FIG. 5. Spectra of methanol in 393 cm long, 150 μm i.d. LCOF and vial acquired with 88 mW of 785 nm excitation in single 0.25-second acquisitions. Absolute peak positions are shown in parentheses. Neither spectrum is corrected for detector response. The region between 2600 and 3200 $cm^{-1}$ is shown in the inset with a magnified ordinate scale.

$$\frac{\eta_S}{\eta_L} = \left(2 - \left(\frac{b_s}{a}\right)^2\right)\left(\frac{b_L}{a}\right)^2 \quad (5)$$

where $\eta_s$ and $\eta_L$ are the coupling efficiencies of the LCOFs whose respective core radii are smaller and larger than that of the GI fiber, $b_s$ and $b_L$ are the core radii of the smaller and larger LCOFs, and $a$ is the core radius of the GI fiber. Evaluating Eq. 5 shows that the coupling efficiency of the 50 μm i.d. LCOF is approximately 4 times greater than that of the 150 μm LCOF. We believe that this factor is consistent with the observed differences in Raman intensity. However, we note that other factors may be involved and that different results should be expected in Raman apparatus having different optical transfer systems.

**Enhancement vs. Wavelength.** Spectra of methanol taken with 785 nm excitation in the same 393 cm long, 150 μm i.d. LCOF and 1.5 m. deep vial used in the 532 nm work are shown in Fig. 5. The larger, lower-loss 150 μm i.d. LCOF was chosen for this work under the assumption that absorption in the liquid core would play a greater role in determining overall waveguide loss than in the case of the smaller 50 μm i.d. LCOF. Both spectra shown in Fig. 5 were obtained with 88 mW of input laser power in a single 0.25-second-long acquisition. The power emitted from the LCOF was 0.5 mW, indicating that the physical length of the LCOF was much greater than its attenuation length and that the loss of the methanol-filled LCOF is considerably higher at 785 nm than at 532 nm. This increase in attenuation has been observed before[22,36] and can be attributed to absorption by high-overtone hydrogen stretching vibrations.

Three differences are immediately apparent when the spectra in Fig. 5 are compared to those in Fig. 4. First, the relative intensities of the methanol peaks change dramatically when the excitation wavelength is shifted from 532 to 785 nm. This is an artifact related to the decrease in CCD quantum efficiency with wavelength. As mentioned above, a detector response curve was unfortunately unavailable for the 785 nm system. Second, comparison of Figs. 4 and 5 indicates that the LCOF provides greater intensity enhancement with 532 nm excitation than with 785 nm excitation. This is almost certainly due to the higher attenuation of methanol-filled LCOFs at 785 nm than at 532 nm. However, because the 532 and 785 nm experiments were performed in different systems it is conceivable that differences in microscope optics have some influence on the observed results. Finally, it is seen in Fig. 5 that the intensity enhancement provided by the LCOF is strongly wavelength dependent. Specifically, the enhancement factors in the 785 nm spectra are 37 at 1033 $cm^{-1}$, 22 at 1450 $cm^{-1}$, and 9 at 2834 and 2943 $cm^{-1}$. By contrast the spectra in Fig. 4 indicate little variation in intensity enhancement.

We attribute the decrease in enhancement over the 785 nm spectrum to the increased loss of the LCOF as the wavelength is increased. The effect of self-absorption on Raman spectral intensity has been studied in detail previously in conjunction with more highly attenuating samples,[39–50] as well as dilute solutions of resonance-enhanced analytes in glass LCOFs.[12,13] Very recently, Song et al.[25] reported 5× greater enhancement of the 1003 $cm^{-1}$ Raman peak in benzene than the 1074 $cm^{-1}$ peak in 0.1 M aqueous $NaHCO_3$ in experiments involving Teflon®-AF LCOFs with 785 nm excitation, and attributed the difference to absorption in the water core. Similarly, in the present case we believe that the differences in intensity enhancement can be attributed to self-absorption by high-overtone vibrational bands of the core liquid. With a comparison of the absolute peak positions of the Raman spectra in Fig. 5 to previously reported loss spectra of methanol in Teflon®-AF-based LCOFs,[36] it can be seen that the 2835 $cm^{-1}$ (1010 nm) and 2942 $cm^{-1}$ (1021 nm) Raman C–H stretching peaks which are least enhanced in the LCOF coincide with the peak of an "intense" loss feature that can most likely be assigned as a C–H overtone combination band.[51] Similarly the 1450 $cm^{-1}$ (866 nm) Raman $CH_3$ bend peak is located at the edge of a weaker absorption feature that can probably be assigned as a third-overtone C–H stretching band.[51] The 1033 $cm^{-1}$ (854 nm) Raman CCO stretch peak that experiences greatest enhancement in the LCOF overlaps with the significantly weaker tail of the same third-overtone C–H band. By analogy with these results it can be assumed that the broad, intense second-overtone OH absorption band centered near 977 nm in water[52] (Raman shift of approximately 2500 $cm^{-1}$ with 785 nm excitation) will more effectively attenuate Raman light in aqueous solutions and potentially render LCOFs less beneficial in this region.

The extent to which self-absorption will complicate analytical measurements in LCOFs will depend on how the optical properties of the core liquid vary between samples. In situations where the core optical characteristics remain approximately constant (analysis of most dilute aqueous solutions, for example), the primary consequence should be performance degradation in certain spectral regions analogous to that already caused by variation in grating and detector efficiency. In quantitative analysis no correction factors should be necessary other than those obtained through routine calibration of the instrument with standard solutions. In qualitative analysis it should be possible to employ relatively straightforward

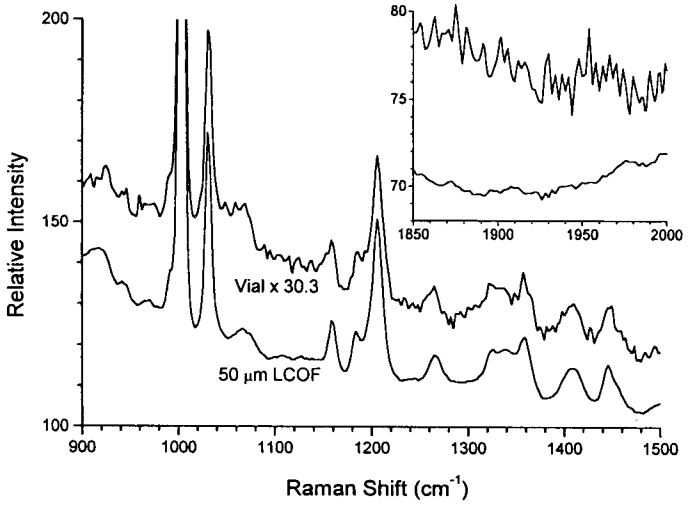


FIG. 6. Spectra of 1% aqueous phenylalanine in vial (sum of three 10-second acquisitions) and 92 cm long, 50 μm i.d. LCOF (sum of 100 0.1-second acquisitions) using 25.7 mW of 532 nm radiation. The former (vial) spectrum was multiplied by 30.3 and offset for comparison. Inset shows relative baseline noise.

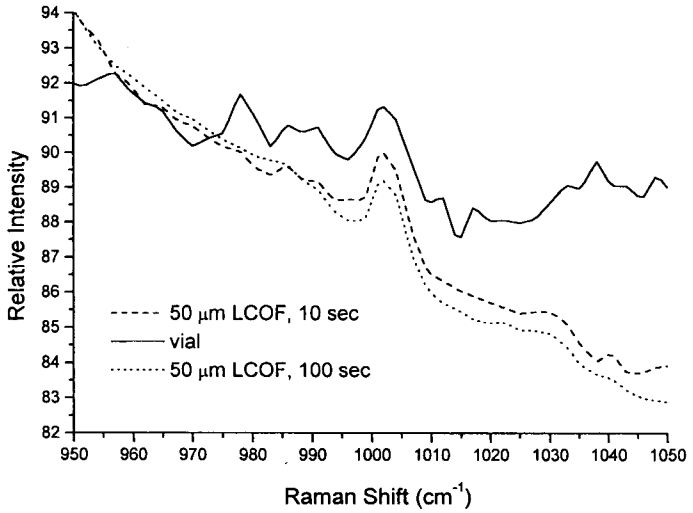


FIG. 7. Spectra of 0.01% aqueous phenylalanine in vial (sum of 16 10-second acquisitions) and 92 cm long, 50 μm i.d. LCOF (10-second and 100-second acquisition times) using 25.7 mW of 532 nm radiation. The intensity of the former (vial) spectrum was multiplied by 5.7 and that of the latter (100-second LCOF) spectrum divided by 9.2 to obtain similar intensity values.

corrections procedures similar to those developed for detector/spectrograph response. However, in both quantitative and qualitative applications where the core optical properties vary significantly between samples (or where the excitation frequency must be changed between samples) the problem of self-absorption becomes more difficult. In these cases it will likely be necessary to introduce well-chosen standards into each sample or to use more complicated correction factors similar to those developed for resonance Raman[43,45] applications.

**Signal-to-Noise Ratio Enhancement.** Figure 6 shows spectra of 1 wt % ($6 \times 10^{-2}$ M) phenylalanine in water acquired by using 25.7 mW of 532 nm radiation in a 92 cm long, 50 μm i.d. Teflon®-AF 2400 LCOF and a vial that provided no enhancement due to waveguiding. The former (LCOF) spectrum is the sum of 100 0.1-second acquisitions, while the latter (vial) spectrum is the sum of three 10-second acquisitions. The spectrum acquired in the vial was multiplied by a factor of 30.3 to make the peak-to-baseline height of the 1004 cm$^{-1}$ ring-breathing peak (shown off-scale in Fig. 6) equal to that of the same peak in the LCOF spectrum. Therefore, the LCOF enhanced the intensity of the phenylalanine spectrum by a factor of approximately 91. It is seen by comparison with Fig. 1 that the section of spectrum shown in Fig. 6 includes the region of most intense Teflon®-AF fluorescence. Nevertheless, it is evident from Fig. 6 that the signal-to-noise ratio of the spectrum acquired in the LCOF is significantly better than that acquired in the vial even though the total acquisition time was a factor of three shorter. The extent of the signal-to-noise improvement can be seen more clearly in the inset of this figure, which shows a section of the spectrum containing no phenylalanine peaks. Although it is not shown in Fig. 6, close inspection of the phenylalanine spectrum shows no evidence of Teflon®-AF Raman peaks in the 700–850 cm$^{-1}$ region.

Spectra of 0.01 wt % ($6 \times 10^{-4}$ M) phenylalanine in water acquired at 532 nm in the same 92 cm long, 50 μm i.d. LCOF and vial used for the 1 wt % phenylalanine measurements are shown in Fig. 7. The spectral region in Fig. 7 was chosen to show the 1004 cm$^{-1}$ phenylalanine ring-breathing peak. The LCOF spectra were obtained under two sets of acquisition conditions (100 0.1-second accumulations and 100 1-second accumulations in which the water OH band was saturated), while the spectrum in the vial was acquired with 16 10-second accumulations. In all cases the incident laser power was 25.7 mW. It is clear once again that signal-to-noise ratios of the spectra acquired in the LCOF are far superior to that of the spectrum acquired in the vial, although the latter involved longer acquisition time. In fact the signal-to-noise ratio is so poor in the spectrum acquired in the vial that conclusive identification of the phenylalanine peak is questionable.

Spectra of 1% phenylalanine acquired by using 86.5 mW of 785 nm radiation in a 41 cm long, 50 μm i.d. Teflon®-AF 2400 LCOF and a vial are shown in Fig. 8. The former (LCOF) spectrum was acquired with 20 0.5-second accumulations, while the latter (vial) spectrum was acquired using a single 20-second accumulation and was further multiplied by a factor of 29 to equalize the peak-to-baseline heights of the 1004 cm$^{-1}$ peaks in the two spectra. In spite of the reduced intensity enhancement at 785 nm and the difference in acquisition times, it is clear from Fig. 8 that the signal-to-noise ratio of the LCOF spectrum is substantially better than that of the spectrum acquired with the vial. Comparing the data in Fig. 8 with those in Fig. 5 also indicates that, as in the case of 532 nm excitation, the 50 μm i.d. LCOF provided greater enhancement than the 150 μm i.d. LCOF. However, the fact that the spectra in Figs. 8 and 5 were acquired by using different core liquids precludes quantitative comparison. (The enhancement at 1004 cm$^{-1}$ calculated from the data in Fig. 8 is approximately 54 based on absolute peak heights or 58 based on peak-to-baseline values. Less enhancement would be expected near the 977 nm absorption band of water; however, phenylalanine lacks Raman bands in this region.)

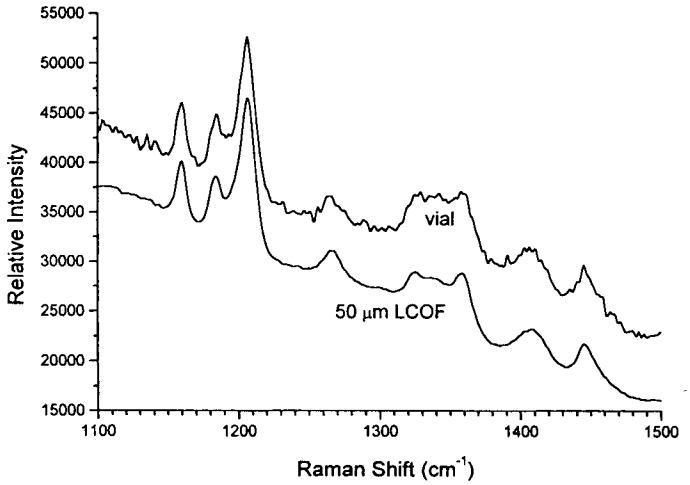


FIG. 8. Spectra of 1% aqueous phenylalanine in vial (one 20-second acquisition) and 41 cm long, 50 μm i.d. LCOF (sum of 20 0.5-second acquisitions) using 86.5 mW of 785 nm laser radiation. The former (vial) spectrum was multiplied by a factor of 29. Neither spectrum is corrected for detector response.

## CONCLUSION

We have investigated several properties of Teflon®-AF 2400 LCOFs with respect to their utility in analytical Raman spectroscopy. Both raw Teflon®-AF pellets and Teflon®-AF capillaries were found to emit photobleachable fluorescence peaking at a shift of approximately 1500 $cm^{-1}$ when excited with 532 nm radiation. The observed fluorescence may contribute to a baseline shift observed in Raman spectra acquired in the LCOFs. However, it does not appear to adversely affect signal-to-noise ratio, and spectra of dilute ($6 \times 10^{-2}$ M and $6 \times 10^{-4}$ M) aqueous phenylalanine acquired in LCOFs were found to have significantly better signal-to-noise ratios than similar spectra acquired in conventional cells.

The dependence of Raman intensity on LCOF length was measured at 532 nm in backscattering geometry with the use of a methanol-filled LCOF and found to agree well with the functional form predicted by Walrafen.[2] The variation in Raman intensity enhancement with LCOF diameter was investigated by using the same core liquid, excitation wavelength, and collection geometry. A maximum intensity enhancement factor of approximately 120 was achieved with a 50 μm i.d. LCOF, while somewhat less enhancement was obtained from a lower loss 150 μm i.d. LCOF. This result was shown to be consistent with the ability of the Kaiser HoloLab 5000 microscope used in this work to more efficiently couple to the small-diameter LCOF. It also emphasizes that the optics of the complete spectroscopic system must be considered if maximum enhancement is to be derived from an LCOF cell.

The effects of excitation and scattering wavelength on intensity enhancement were investigated with the use of 150 μm i.d. LCOFs filled with methanol. Enhancement factors in 532 nm-excited spectra were found to be constant over the measured spectral region, while those in 785 nm-excited spectra were found to vary in a manner consistent with absorption by high-overtone vibrational bands in the core liquid. In analytical applications where the optical properties of all samples are similar, it is likely that spectral distortion due to overtone absorption can be corrected through straightforward procedures similar to those already used to account for variations in detector and spectrograph response. However, in situations where the core optical properties vary significantly between samples (or where the excitation frequency must be changed between samples), it will likely be necessary to introduce well-chosen standards into each sample or use more complicated correction factors similar to those developed for resonance Raman[43,45] applications.

On the basis of the observed intensity and signal-to-noise ratio enhancements, we believe that Teflon®-AF 2400 LCOFs should be well suited to use in biological, environmental, or other applications where factors such as small scattering cross sections, sensitivity to laser power, low analyte concentrations, and/or rapid sampling requirements mandate the use of nonstandard sampling techniques. The small volume (two microliters per linear meter) of the 50 μm i.d. LCOFs in particular should make them attractive for use in HPLC or other techniques where sample volume is limited.


### ACKNOWLEDGEMENT

This work was supported by the National Science Foundation under Grant no. DMI-9705611.



1. G. E. Walrafen and J. Stone, Appl. Spectrosc. **26,** 585 (1972).
2. G. E. Walrafen, Phys. Bl. **12,** 540 (1974).
3. G. E. Walrafen, Appl. Spectrosc. **29,** 179 (1975).
4. G. E. Walrafen, Appl. Spectrosc. **31,** 295 (1977).
5. W. J. Schmid and H. W. Schrotter, J. Raman Spectrosc. **10,** 212 (1981).
6. H. B. Ross and W. M. McClain, Appl. Spectrosc. **35,** 439 (1981).
7. Z. Li, Y. Zhao, X. Sun, L. Pei, D. Li, Q. Cui, and S. Liang, Chinese Phys. **12,** 394 (1992).
8. Z. Li, T. Chang, X. Sun, L. Pei, and S. Gao, Chin. Phys. Lett. **10,** 409 (1993).
9. Z. Li, W. Xu, X. Sun, L. Pei, Y. Ren, C. Pu, and S. Gao, Acta Opt. Sin. **13,** 999 (1993).
10. S. Gao, Z. Li, X. Sun, and W. Zhang, Chem. J. Chin. Univ. **18,** 457 (1997).
11. S. Gao, Z. Li, J. Li, and W. Zhang, Chin. J. Lasers Part A **24,** 738 (1997).
12. S. Gao, Z. Li, J. Li, and W. Zhang, Acta Opt. Sin. **17,** 1319 (1997).
13. Z. Li, J. Li, and S. Gao, Jpn. J. Appl. Phys. **37,** 1889 (1998).
14. J. H. Lowry, J. S. Mendlowitz, and N. S. Subramanian, Opt. Eng. **31,** 1982 (1992).
15. K. Hong and L. W. Burgess, Proc. SPIE **2293,** 71 (1994).
16. S. J. Mackenzie and J. P. Dakin, Proc. Conf. Lasers and Electro-Optics Europe 206 (1996).
17. P. Dress and H. Franke, Proc. SPIE **2686,** 157 (1996).
18. P. Dress, and H. Franke, Appl. Phys. Part B **63,** 12 (1996).
19. P. Dress, and H. Franke, Rev. Sci. Instrum. **68,** 2167 (1997).
20. R. Altkorn, I. Koev, and A. Gottlieb, Appl. Spectrosc. **51,** 1554 (1997).
21. P. K. Dasgupta, Z. Genfa, S. K. Poruthoor, S. Caldwell, S. Dong, and S. Y. Liu, Anal. Chem. **70,** 4661 (1998).
22. R. Altkorn, I. Koev, R. P. Van Duyne, and M. Litorja, Appl. Opt. **36,** 8992 (1997).
23. R. D. Waterbury, W. Yao, and R. H. Byrne, Anal. Chim. Acta **357,** 99 (1997).
24. W. Yao and R. H. Byrne, Talanta **48,** 277 (1999).
25. L. Song, S. Liu, V. Zhelyaskov, and M. A. El-Sayed, Appl. Spectrosc. **52,** 1364 (1998).
26. C. Gooijer, G. P. Hoornweg, T. de Beer, A. Bader, D. J. van Iperen, and U. A. T. Brinkman, J. Chromatography A **824,** 1 (1998).
27. D. Marcuse, *Principles of Optical Fiber Measurements* (Academic Press, San Diego, California, 1981).
28. H. Owen, D. E. Battey, M. J. Pelletier, and J. B. Slater, Proc. SPIE **2406,** 260 (1995).

29. H. Owen, J. M. Tedesco, and J. B. Slater, U.S. Patent 5,377,004 (1994).
30. M. J. Pelletier, J. Slater, K. L. Davis, W. K. Kowalchyk, and I. R. Lewis, Proc. Microsc. Microanal. **3,** 823 (1997).
31. D. E. Battey, J. B. Slater, R. Wludyka, H. Owen, D. M. Pallister, and M. D. Morris, Appl. Spectrosc. **47,** 1913 (1993).
32. D. E. Battey, H. Owen, and J. M. Tedesco, U.S. Patent 5,559,597 (1996).
33. C. Shen, T. J. Vickers, and C. K. Mann, Appl. Spectrosc. **46,** 772 (1992).
34. A. W. Fountain III, T. J. Vickers, and C. K. Mann, Appl. Spectrosc. **52,** 462 (1998).
35. C. D'Ambrosio, H. Leutz, M. Taufer, T. Shimizu, O. Shinji, and J. Sun, Nucl. Instrum. Meth. Phys. Res. Sect. A **306,** 549 (1991).
36. R. Altkorn, J. Near Infrared Spectrosc. **5,** 35 (1997).
37. P. Di Vita and R. Vannucci, Appl. Opt. **15,** 2765 (1976).
38. F. Tosco, *Fiber Optic Communications Handbook* (TAB Books, Blue Ridge Summit, Pennsylvania 1990), 2nd ed.
39. E. R. Lippincott, J. P. Sibilia, and R. D. Fisher, J. Opt. Soc. Amer. **49,** 83 (1959).
40. B. Schrader and G. Bergmann, Z. Anal. Chem. **225,** 230 (1967).
41. R. J. Gillespie and M. J. Morton, J. Mol. Spectrosc. **30,** 178, (1969).
42. T. C. Strekas, D. H. Adams, A. Packer, and T. G. Spiro, Appl. Spectrosc. **28,** 324 (1974).
43. M. Ludwig and S. A. Asher, Appl. Spectrosc. **42,** 1458 (1988).
44. G. Turrell, "Raman Sampling", in *Practical Raman Spectroscopy,* D. J. Gardiner and P. R. Graves, Eds. (Springer, New York, 1989).
45. T. J. Vickers, C. K. Mann, J. Zhu, and C. K. Chong, Appl. Spectrosc. Rev. **26,** 341 (1991).
46. B. Schrader, A. Hoffmann, and S. Keller, Spectrochim. Acta Part A **47,** 1135 (1991).
47. C. J. Petty, Vib. Spectrosc. **2,** 263 (1991).
48. J. J. Laserna, L. M. Cabalin, and R. Montes, Anal. Chem. **64,** 2006 (1992).
49. D. N. Waters, Spectrochim. Acta, Part A **50,** 1833 (1994).
50. N. Everall, J. Raman Spectrosc. **25,** 813 (1994).
51. A. S. Bonanno and P. R. Griffiths, J. Near Infrared Spectrosc. **1,** 13 (1993).
52. C. K. N. Patel and A. C. Tam, Nature **280,** 302 (1979).